Effects of Carbonaceous Nanofillers on the Mechanical and Electrical Properties of Crosslinked Poly(Cyclooctene)

A. Dorigato, A. Pegoretti
Department of Industrial Engineering and INSTM Research Unit, University of Trento, Trento 38123, Italy

In this work the mechanical and electrical behavior of poly(cyclooctene) (PCO)-based nanocomposites were investigated. At this aim, different amounts (0.5–4 wt%) of carbon black (CB), carbon nanofibers (NF) and exfoliated graphite nanoplatelets (xGnP) were melt compounded with a PCO matrix and crosslinked with dicumylperoxide (DCP). The progressive increase of the DCP concentration led to an evident decrease of both the melting temperature and the crystallization temperature, and also the relative crystallinity was strongly reduced. Microstructural observations on nanocomposites materials with a DCP amount of 2 wt% evidenced how CB nanocomposites were characterized by a good nanofiller dispersion within the matrix, while NF and xGnP nanofilled samples presented a more aggregated morphology. The introduction of CB and xGnP determined an enhancement of the elastic modulus of the material, without impairing the ultimate properties of the pristine matrix. Electrical resistivity measurements evidenced how the prepared composites can be interesting as electro-active materials for CB concentrations higher than 2 wt%. POLYM. ENG. SCI., 57:537–543, 2017. © 2016 Society of Plastics Engineers

INTRODUCTION

The introduction of conductive nanofillers could dramatically increase the electrical conductivity of the resulting materials [1–3]. The electrical behavior of these systems can be successfully explained considering the percolation theory [4]. After a given filler concentration (i.e., the percolation threshold), the conductive nanofiller forms a continuous network through the insulating matrix and the resistivity could be therefore decreased by several orders of magnitude. For instance, in some works of our group, the thermo-mechanical properties and the electrical monitoring capability of an epoxy matrix nanomodified with different amounts of CB and NF was investigated [5, 6].

Conductive nanofillers can be also exploited for the preparation of electro-active shape memory polymers (SMP). SMPs have the peculiar property of "remembering" their original shape to which they return when subjected to external stimuli (heat, light, electric and magnetic fields) [7, 8]. Moreover, the demand to avoid external heaters has led to a new generation of electrically conducting SMPs filled with carbon nanotubes [9, 10], carbon particles [11, 12], conductive fiber [13], and nickel zinc ferrite ferromagnetic particles, etc. [11, 14]. Therefore, several examples of electro-activated polymeric composites have already been reported in the open literature [15–18], and it has been demonstrated that the addition of electrically conductive and/or magnetic nanoparticles in a polymer matrix leads to complete shape recovery of the sample upon the application of an electric or magnetic field [19].

Among shape memory polymeric system, some attention was devoted in the past to poly(cyclooctene) (PCO), which is a polyolefinic material characterized by the presence of an hydrocarbon backbone containing both cyclic and linear structures. This matrix can be synthesized starting from cyclooctene, that can be obtained from the 1,3-butadiene and 1,5-cyclooctadiene through a metathesis reaction. In this way, both cyclic and linear structures can be formed [20]. The cis/trans ratio determines the crystallinity degree, and it can be controlled by varying the polymerization conditions. From a mechanical point of view, PCO is a thermoplastic material with an elastomeric behavior, and its applicability is often limited by the low melting temperature (i.e., slightly above ambient temperature). Therefore, a crosslinking process is often required to improve the mechanical response of the material [21]. The most diffused method for the PCO crosslinking is the chemical crosslinking with dicumylperoxide [22, 23]. In this way, it is possible to improve the dimensional stability of the material at elevated temperatures and therefore to increase the mechanical performances. Above the melting temperature, crosslinked PCO behaves like a noncrystalline elastomer. Because of its peculiar properties, PCO finds application in tyres production, in the rubber recycling process and as toughening and sound adsorbing agent in the asphalt.

In the last years the investigation of the physical properties of PCO-based nanocomposites is rather limited, and the greatest part of the papers in literature is focused on the optically and magnetically shape memory behavior [7, 24, 25]. For instance, Cuevas et al. investigated the shape memory properties of PCO composites filled with ferromagnetic particles. In that case, the thermal activation of the composites was obtained through the application of a magnetic field [26]. Kunzelman et al. monitored the shape memory behavior of PCO through chromogenic and fluorescent molecules [27]. Quite surprisingly, no papers dealing with the electro-active shape memory behavior of PCO nanocomposites can be found in the open literature.

Taking into account these considerations, the objective of the present work is that to characterize the thermal, mechanical and electrical properties of PCO-based nanocomposites filled with different kinds of carbon-based nanofillers (xGnP, CB, and NF), potentially applied as electro-active shape memory materials. After a preliminary characterization of the neat matrix filled with different amounts of DCP, the attention was focused on the macroscopic properties of the resulting composites, with particular attention to the correlation between their microstructural and electrical behavior.

EXPERIMENTAL

Materials

Polymeric granules of a Vestenamer 8012®, supplied by Degussa, were utilized as PCO matrix (weight average molecular weight $M_w = 90000$, melting temperature $T_m = 65°C$, cis/

Correspondence to: A. Dorigato; e-mail: andrea.dorigato_1@unitn.it
DOI 10.1002/pen.24449
Published online in Wiley Online Library (wileyonlinelibrary.com).

TABLE 1. List of the prepared samples.

Sample	DCP content (wt%)	Nanofiller content (wt%)
PCO_DCP_0.25	0.25	
PCO_DCP_0.5	0.5	
PCO_DCP_1	1	
PCO_DCP_2	2	
PCO_DCP_3	3	
PCO_DCP_2_CB_0.5	2	0.5
PCO_DCP_2_CB_1		1
PCO_DCP_2_CB_2		2
PCO_DCP_2_CB_4		4
PCO_DCP_2_NF_0.5	2	0.5
PCO_DCP_2_NF_1		1
PCO_DCP_2_NF_2		2
PCO_DCP_2_NF_4		4
PCO_DCP_2_xGnP_0.5	2	0.5
PCO_DCP_2_xGnP_1		1
PCO_DCP_2_xGnP_2		2
PCO_DCP_2_xGnP_4		4

trans ratio 20/80, density 0.91 g/cm^3). DCP powder, provided by Sigma-Aldrich, was utilized as radicalic crosslinker (purity 98%). Ketjenblack EC600JD carbon black nanoparticles were supplied by Akzo Nobel Chemicals Spa (Arese, Italy). This nanofiller is constituted by fine aggregates of spherical particles with typical dimension of around 30 nm and a density of 1.95 g/cm^3. The specific surface area (SSA) of CB nanoparticles, measured following BET procedure, was 1,353 m^2/g. Vapor grown carbon nanofibers (1195JN) have been supplied by NanoAmor Inc. (Houston, USA). These fibers (density = 1.78 g/cm^3, SSA = 28.8 m^2/g) have a length of 5–40 nm, a core diameter of 0.5–10 nm and an outside diameter of 240–500 nm. Exfoliated graphite nanoplatelets (density = 2.05 g/cm^3, purity = 97 wt%) were provided by XG Science Inc. (East Lansing, USA). All the materials were used as received.

Preparation of the Samples

Bulk samples were prepared through a melt compounding process by using a Thermo Haake Reomix 600p compounder. PCO granules and DCP were mixed at 70°C for 5 min at a rotor speed of 60 rpm. Nanofiller was then introduced in the compounding chamber, and the mixture was compounded for other 5 min. The parameters of the compounding process were determined after a preliminary characterization activity. The aim of the compounding process was that to obtain a good nanofiller dispersion without activating the crosslinking process. The resulting materials were then hot pressed through a Carver laboratory press at 180°C for 30 min. The pressing time was chosen in order to complete the crosslinking process of the samples. In this way, square sheets of the neat PCO matrix with different DCP amounts and nanocomposites samples at different concentrations, with a mean thickness of 1 mm, were produced. Table 1 summarizes the list of the prepared samples.

Experimental Techniques

The first part of the characterization activity was focused on the effect of the DCP addition on the thermo-mechanical properties of the PCO matrix. Thermal properties of the samples (i.e., melting temperature [T_m], crystallization temperature [T_c], crosslinking temperature [T_{cr}], crystallinity degree [χ]) were evaluated through differential scanning calorimetry (DSC) tests, performed with a Mettler DSC30 apparatus (Schwerzenbach, Switzerland). After a thermal cycle from −50 to 280°C at a heating rate of 10°C/min, a cooling stage up to −50°C followed by a second heating at 280°C under an air flow of 100 ml/min, were carried out.

In order to evaluate the gel content of the compounded materials, the evaluation of the insoluble residue was conducted. At this aim, neat PCO samples with different amounts of DCP were immersed in toluene at 60°C for 12 h. The resulting samples were then put in an oven under vacuum at 50°C for 8 h. The gel content (GC) was determined as the ratio between the mass of the samples after (m_p) and before (m_i) the solubilization, as reported in *Eq. 1*

$$GC\ (\%) = \left(\frac{m_p}{m_i}\right) \times 100 \quad (1)$$

Quasi-static tensile properties were evaluated at 20°C through an Instron 4502 tensile testing machine equipped with a load cell of 1 kN on 1BA dumbbell specimens. The specimens were obtained from the prepared sheets through punch-cut operations. Tensile tests for the evaluation of the elastic modulus (E) were conducted at a testing speed of 0.25 mm/min and the deformation was recorded through a resistance extensometer with a gauge length of 12.5 mm, while tensile properties at yield (σ_y) and at break (σ_b, ε_b) were evaluated at a speed of 50 mm/min without using the extensometer. At least five specimens were tested for each composition.

Morphology of the cryofractured surfaces of the nanofilled samples was investigated through a Zeiss Supra 40 field emission scanning electronic microscope (FESEM), at an acceleration voltage of about 1 kV and a pressure of 10^{-6} Torr. The surfaces of the samples were metalized with a silver paste before the observations.

Electrical bulk resistance measurements on the nanofilled samples were performed at room temperature in direct current mode. A 6 1/2-digit electrometer/high resistance system, supplied by Keithley Instruments Inc. (Cleveland, Ohio, USA), was used. Because of the high electrical resistance of the samples and the relatively low contact resistance, a 2-point electrical measurement was chosen as test configuration. In order to decrease the contact resistance, the sample surfaces in contact with the electrodes were painted with a silver coating. Measurements were carried out on rectangular punch-cut samples (cross section of 5 mm × 1 mm, length of 100 mm), and at least five specimens were tested for each composition. When the electrical resistance was lower than 10^5 Ω, measurements were carried out under an applied voltage of 10 V, and the resistance values were measured after a time lapse of 60 s, in order to minimize time-dependent effects. When the electrical resistance was between 10^5 and 10^{12} Ω, measurements were carried out under an applied voltage of 100 V. When the electrical resistance was higher than 10^{12} Ω, measurements with an applied voltage of 1,000 V were taken on square film samples (length of 95 mm and thickness of 1 mm). In this latter case coaxial electrodes were used in order to minimize the amount of current flowing through the surface.

 DOI 10.1002/pen

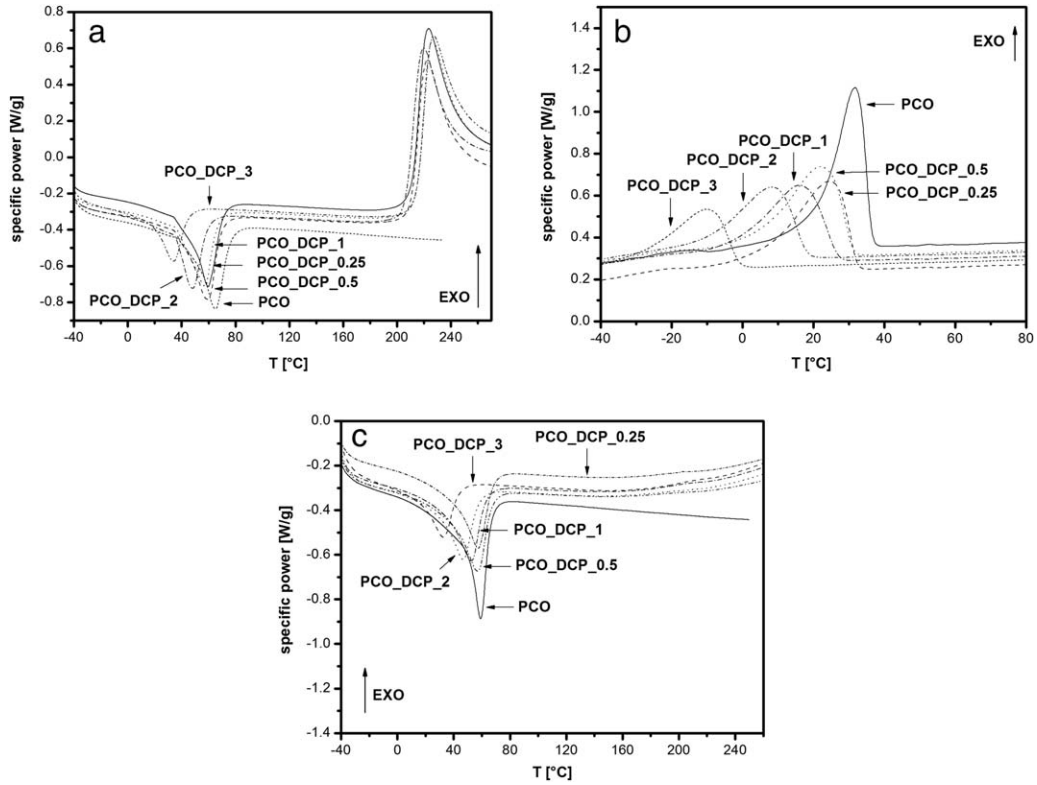

FIG. 1. DSC thermograms of neat PCO with different DCP amounts. (a) First heating scan, (b) cooling scan, and (c) second heating scan.

RESULTS AND DISCUSSION

Physical Properties of the PCO Matrix

The first part of the work was focused on the analysis of the thermal properties of the neat PCO, in order to evaluate the influence of the crosslinker (DCP) amount on the melting and crystallization behavior of the material. In Fig. 1a the first heating scan of the DSC thermograms of neat PCO and of the samples with various DCP amounts are reported, while the most important results are summarized in Table 2. It can be noticed the presence of a single endothermic signal (i.e., melting peak), and the melting temperature decreases with the DCP amount. Also, the peak area is noticeably decreased upon crosslinker addition. For instance, melting temperature and relative crystallinity degree of neat PCO are respectively 63.0°C and 34.9%, while by adding a PCO amount of 3 wt% T_{f1} is decreased of 30°C, and the crystalline amount is reduced at 18.9%. This means that DCP introduction is responsible of a noticeable decrease of the melting temperature and of the crystallinity degree of the polymer matrix. This result is in agreement to what commonly observed for chemically crosslinked polymers [23, 28–30]. Specifically, at elevated peroxide amounts spherulites formation and growth is hindered by the presence of DCP. It is evident that this effect will strongly affect the mechanical properties and the thermal stability of the resulting materials. The exothermic peak reported in Fig. 1a at temperatures above 200°C can be attributed to the unreacted fraction of DCP.

Also, the crystallization temperature is strongly reduced upon DCP addition (up to −10°C with a DCP amount of 3 wt% [see Fig. 1b and Table 2]), and similar conclusions can be drawn also considering the second heating scan (see Fig. 1c).

In order to assess the effect of the DCP addition on the gel content of PCO, an estimation of the amount of nonlinked macromolecules was performed by solvent removal, and the most important results are summarized in Fig. 2. The gel content increases with the DCP amount, reaching a plateau at a DCP content of 2 wt%. It is clear that at elevated crosslinking amounts, the molecular mobility is strongly reduced, and therefore a considerable increase of the DCP concentrations should be required to obtain a further crosslinking of the material [22, 23, 28, 31, 32].

In Table 3, the results of the quasi-static tensile tests on PCO samples with different DCP amounts are reported. As it

TABLE 2. Results of DSC tests on neat PCO samples with different DCP amounts.

Sample	T_{f1} (°C)	T_{cr} (°C)	T_c (°C)	T_{f2} (°C)	χ_{f1} (%)	χ_c (%)	χ_{f2} (%)
PCO	63.0		31.7	59.2	34.9	31.4	33.0
PCO_DCP_0.25	59.7	223.5	24.7	57.3	33.6	27.1	27.8
PCO_DCP_0.5	59.2	222.7	21.7	57.0	33.9	25.8	29.4
PCO_DCP_1	57.3	226.7	16.2	54.0	30.0	23.7	26.9
PCO_DCP_2	48.3	219.8	8.4	46.7	28.1	21.7	24.2
PCO_DCP_3	33.5	227.2	−10.0	32.8	18.9	16.1	16.8

T_{f1}, melting temperature from the first heating scan of DSC tests; T_{cr}, crosslinking temperature from the first heating scan of DSC tests; T_c, crystallization temperature from the cooling scan of DSC tests; T_{f2}, melting temperature from the second heating scan of DSC tests; χ_{f1}, crystallinity degree from the first heating scan of DSC tests; χ_c, crystallinity degree from the cooling scan of DSC tests; χ_{f2}, crystallinity degree from the second heating scan of DSC tests.

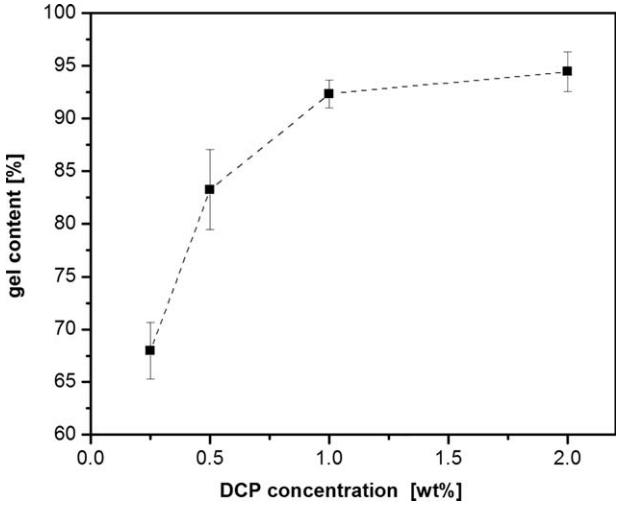

FIG. 2. Gel content of the PCO matrix as a function of the DCP content from insoluble residue evaluation.

could be expected, an increase of the DCP amount leads to a strong drop of the elastic modulus (E), because of the crystallinity decrease detected in DSC tests. For the same reason, also the stress at yield (σ_y) is slightly impaired upon DCP introduction. It is also important to underline that the increase of the gel content at elevated DCP amounts is responsible of the observed decrease of the ultimate properties of the materials (σ_b and ε_b). Consequently, also the specific tensile energy to break (TEB) values are considerably lower at elevated DCP amounts.

Considering that the results of the present work are propedeutical for a future preparation of electro-active shape memory devices, it is important to perform a preliminary selection of the most promising formulations. An increase of the gel content of the materials can be important in order to have a good dimensional stability of the material above the transition temperature (i.e., melting temperature of PCO). On the other hand, the electrical activation of the SMP can be performed only by heating the samples above the ambient temperature through the application of an electrical voltage. DSC tests revealed how with a DCP amount of 3 wt% the melting temperature is about 33.5°C, too near to the room temperature. Moreover, the strong reduction of crystallinity degree experienced with the same DCP content leads to an unacceptable loss of mechanical performances. Therefore, a good compromise seems to be found by choosing a DCP content of 2 wt%. In this way, it is possible to reach a good gel content (about 92%) with an acceptable reduction of the mechanical performances at ambient temperature. Consequently, nanocomposite samples were prepared by taking a constant DCP amount of 2 wt%.

Physical Properties of PCO-Based Nanocomposites

It is well known that the mechanical and the electrical behavior of nanocomposite samples is directly influenced by the dispersion state of the nanofiller within the matrix. In Fig. 3a–c FESEM images of the fracture surfaces of the prepared nanocomposites with a constant nanofiller amount of 4 wt% are represented. As often reported in the scientific literature, the microstructure of CB nanocomposite systems is characterized by the presence of primary particles arranged in aggregates and agglomerates, homogeneously distributed within the polymer matrix (Fig. 3a). This nanocomposites are characterized by the presence of tiny and pale primary particles with average diameter of about 40 nm, organized in agglomerates of about 500 nm. NF filled nanocomposites exhibit a completely different microstructure. In fact, it is possible to detect the presence of single nanofiber with a mean diameter of about 80 nm with a non homogeneous distribution within the polymer matrix (Fig. 3b). According to the electrical percolation theory [4], this morphological feature could negatively affect the electrical conductive behavior of the material. In the case of xGnP-based nancomposites, nanoplatelets are arranged in stacks with a mean thickness of about 80 nm (Fig. 3c). However, a nonoptimal spatial distribution of the nanoplatelets was obtained, and in some micrographs (not reported for the sake of brevity), some stacks 700 nm thick were detected.

It is also important to evaluate the effect of the nanofiller addition to the thermal transitions of the PCO matrix. In Fig. 4a and b the melting temperature (T_m) and the crystallinity degree (χ) of the prepared nanocomposites are, respectively, reported. It can be seen that xGnP addition at concentrations higher than 2 wt% leads to a slight increase of the melting temperature, while CB and NF seems to marginally affect the T_m of the prepared materials. From Fig. 4b it is difficult to find a clear trend of the crystallinity with the nanofiller amounts. However, relatively small differences can be observed. It can be therefore concluded that the nanofiller addition plays a marginal role on the thermal properties of the nanofilled samples. Similar conclusions were drawn in DSC tests reported in our previous work on polyethylene-based nanocomposites [4].

It is well known that the mechanical properties of polymeric materials are largely determined by their thermal properties. Therefore, quasi-static tensile tests were performed on the resulting nanocomposites. In Fig. 5a–d, the trends of the most important tensile properties are reported, while the numerical results are summarized in Table 3. As it usually happens with nanofilled polymers [19, 33–35], an increase of the materials stiffness with the nanofiller amount can be observed, and the best results can be obtained by using exfoliated graphite nanoplatelets (see Fig. 5a). For instance, with an xGnP amount of 4 wt% it is possible to observe a stiffness increase of about three

TABLE 3. Quasi-static tensile properties of PCO samples with different DCP amounts ($T = 20$°C).

Sample	E (MPa)	σ_y (MPa)	ε_b (%)	σ_b (MPa)	TEB (MJ/m^3)
PCO	116.1 ± 10.9	6.36 ± 0.06	1305.2 ± 45.4	14.91 ± 0.86	125.9 ± 5.2
PCO_DCP_0.25	108.7 ± 11.1	7.61 ± 0.10	1422.8 ± 60.5	17.46 ± 0.71	150.1 ± 8.8
PCO_DCP_0.5	71.9 ± 11.8	7.14 ± 0.18	1066.4 ± 53.2	14.02 ± 0.73	108.6 ± 9.2
PCO_DCP_1	49.7 ± 12.5	6.19 ± 0.06	975.2 ± 97.6	13.52 ± 0.67	81.6 ± 4.3
PCO_DCP_2	28.9 ± 4.9	4.46 ± 0.04	597.9 ± 50.7	8.79 ± 0.82	31.8 ± 4.6

DOI 10.1002/pen

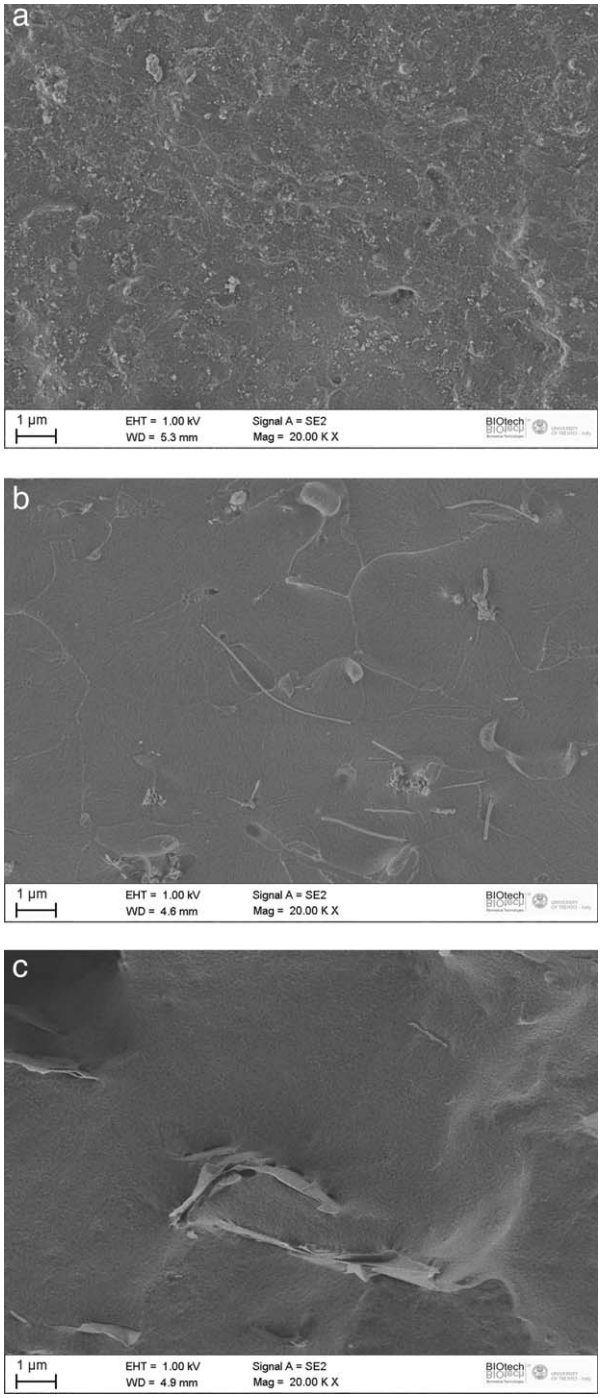

FIG. 3. FESEM images of the PCO-based nanocomposites. (a) PCO_DCP_2_CB_4, (b) PCO_DCP_2_NF_4, and (c) PCO_DCP_2_xGnP_4 samples.

times with respect to the unfilled matrix. This nanofiller is also able to promote an increase of the stress at yield (σ_y) values, while the introduction of both CB and NF does not seem to play any effect on the yield strength of the samples (see Fig. 5b). On the other hand, the introduction of xGnP negatively affects the ultimate properties of the material, with a sensible drop of both the stress (σ_b) and strain (ε_b) at break. It is also interesting to note that the fracture toughness of the neat matrix can be substantially retained introducing both NF and CB even at elevated concentrations (see Fig. 5c and d). The embrittling effect due to xGnP addition is strictly connected to the non optimal distribution of the nanofiller within the matrix (see Fig. 3). It has been noticed how DCP addition can affect the melting temperature and the gel content (i.e., the crystallinity degree) of the material (see Fig. 2). These properties could profoundly modify both the thermal and the mechanical response of the material. On the same way, it could be hypothesized that also nanofiller addition could alter both the melting temperature and/or the gel content of the PCO matrix and that the observed trends in the mechanical properties of nanofilled samples are partially due to a change in the melting temperature or in the crosslinking degree. These aspects will be better analyzed in a future work on these systems.

The possibility of an electrical activation of SMP is strictly related to the possibility to heat them by Joule effect which mostly depends on their electrical conductivity. Therefore, the evaluation of the electrical resistance of the prepared samples is of crucial importance for their possible application as electro-active SMPs. In Fig. 6 the trends of electrical resistivity of the prepared nanocomposites are represented. The electrical resistivity of the neat matrix is of about 10^{17} Ω.cm, in the range typically reported for insulating polymeric materials. The addition of both NF and CB nanoparticles seems to only marginally affect the electrical behavior of the materials even at the highest filler concentrations of 4 wt%. On the

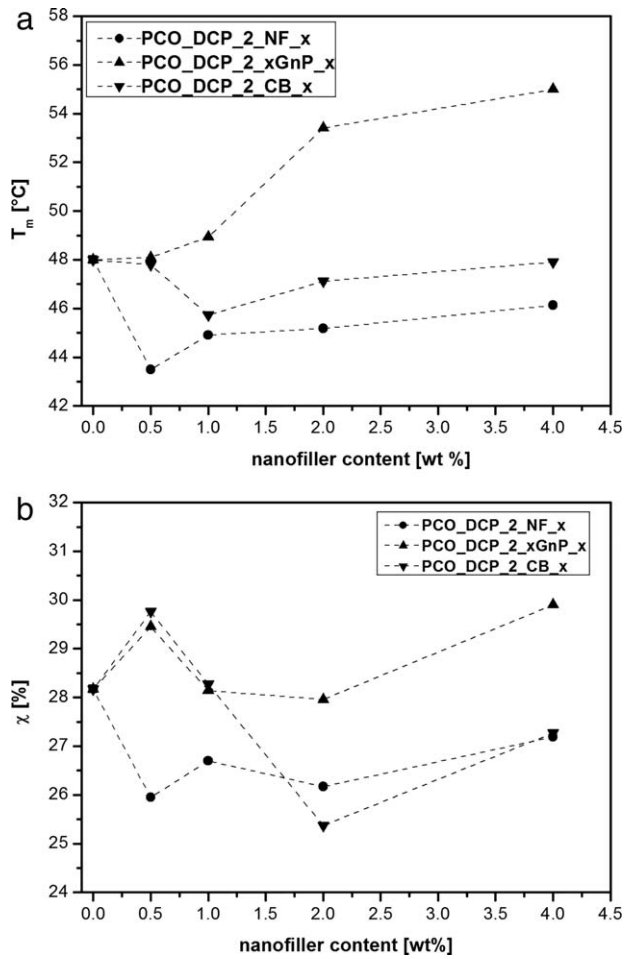

FIG. 4. Results of DSC tests on neat PCO and relative nanocomposites (DCP amount of 2 wt%, first heating scan). (a) Melting temperature and (b) crystallinity degree ($x = 0.5$–4 wt%).

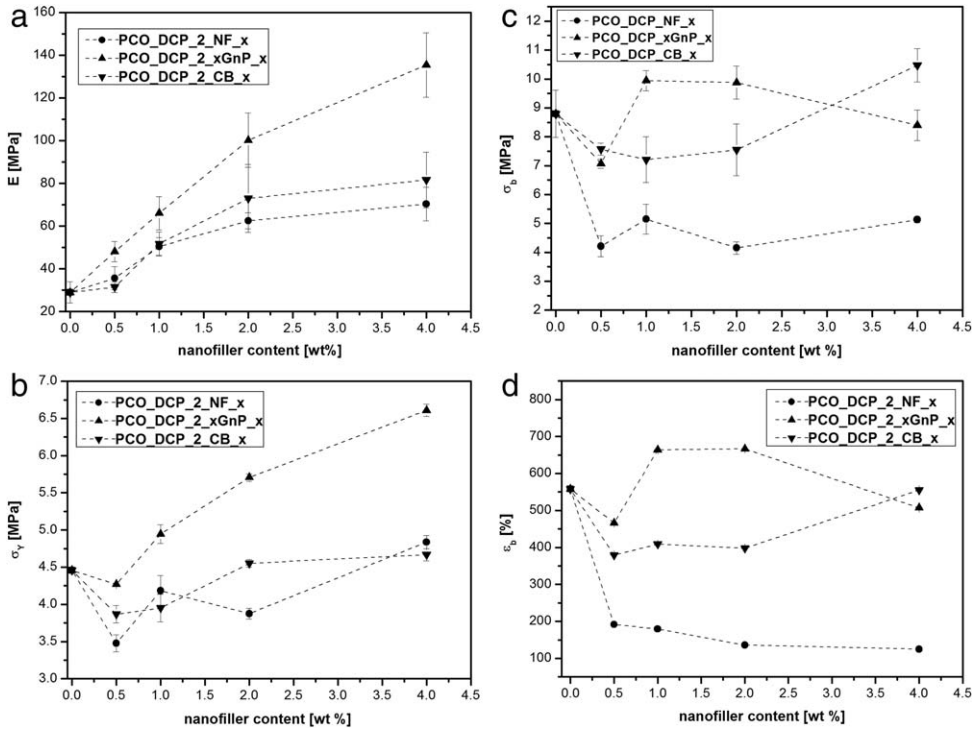

FIG. 5. Results of quasi-static tensile tests on neat PCO and relative nanocomposites (DCP amount of 2 wt%). (a) Elastic modulus, (b) stress at yield, (c) stress at break, and (d) deformation at break ($x = 0.5$–4 wt%).

contrary, by using CB nanoparticles it is possible to observe a strong decrease of the electrical resistivity above the percolation threshold (i.e., for filler contents higher than 1 wt%). With a CB amount of 4 wt%, it is possible to reach a resistivity value of 1.4 10^6 Ω.cm. This result could be explained considering the better nanofiller distribution observed for CB nanocomposites (see Fig. 3). On the basis of the obtained results and on our previous papers on electrically conductive epoxy-based nanocomposites [19], it can be concluded that only CB nanocomposite samples with a nanofiller amount higher than 2 wt% can be potentially applied as electroactive shape memory materials. With these compositions, it is also possible to increase the stiffness of the material without impairing its failure properties.

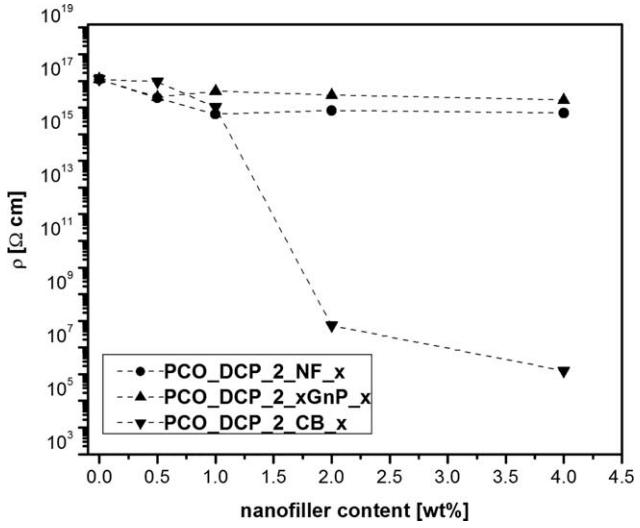

FIG. 6. Electrical bulk resistivity of neat PCO and relative nanocomposites (DCP amount 2 wt%) ($x = 0.5$–4 wt%).

CONCLUSIONS

The objective of the present work was that to investigate the physical properties of PCO-based nanocomposites as potential candidates as electro-activated shape memory devices. At this aim, carbon black, carbon nanofibers and exfoliated graphite nanoplatelets were melt compounded at different concentrations with a PCO matrix and crosslinked with dicumylperoxide (DCP) as a crosslinker.

The preliminary characterization on the PCO matrix showed how the increase of the DCP content was responsible of an evident decrease of the melting temperature, of the crystallization temperature and of the relative crystallinity degree, while the gel content reached a plateau values for DCP contents higher than 2 wt%. Consequently, the mechanical properties of PCO at ambient temperature were negatively affected by DCP introduction. Microstructural observations on the nanocomposites prepared with a DCP amount of 2 wt% evidenced how CB filled samples were characterized by an homogeneous nanofiller dispersion within the matrix, while NF and xGnP nanocomposites presented a more aggregated microstructure. CB introduction could also positively affect the material stiffness, without impairing the yield and the fracture strength. Electrical resistivity measurements evidenced how only CB nanocomposites with a nanofiller amount higher than 2 wt% show conductivity values suitable for the electrical activation of the samples.

ACKNOWLEDGMENTS

Simone Brazzo is gratefully acknowledged for his support to the experimental work.

 DOI 10.1002/pen

REFERENCES

1. Z.J. Fan, C. Zheng, T. Wei, Y.C. Zhang, and G.L. Luo, *Polym. Eng. Sci.*, **49**, 2041 (2009).
2. J. Li, P.S. Wong, and J.K. Kim, *Mater. Sci. Eng. A*, **483–484**, 660 (2008).
3. J. Sumfleth, S.T. Buschhorn, and K. Schulte, *J. Mater. Sci.*, **46**, 659 (2010).
4. M. Traina, A. Pegoretti, and A. Penati, *J. Appl. Polym. Sci.*, **106**, 2065 (2007).
5. D. Pedrazzoli, A. Dorigato, and A. Pegoretti, *J. Nanosci. Nanotechnol.*, **12**, 4093 (2012).
6. D. Pedrazzoli, A. Dorigato, and A. Pegoretti, *Composites, Part A*, **43**, 1285 (2012).
7. A. Lendlein and S. Kelch, *Angew. Chem. Int. Ed.*, **41**, 2034 (2002).
8. R. Bogue, *Assem. Autom.*, **29**, 214 (2009).
9. J.W. Cho, J.W. Kim, Y.C. Jung, and N.S. Goo, *Macromol. Rapid Commun.*, **26**, 412 (2005).
10. I.H. Paik, N.S. Goo, Y.C. Jung, and J.W. Cho, *Smart Mater. Struct.*, **15**, 1476 (2006).
11. H. Koerner, G. Price, N. Pearce, M. Alexander, and R.A. Vaia, *Nat. Mater.*, **3**, 115 (2004).
12. B. Yang, W.M. Huang, C. Li, L. Li, and J.H. Chor, *Scr. Mater.*, **53**, 105 (2005).
13. J.S. Leng, H.B. Lv, Y.J. Liu, and S.Y. Du, *Appl. Phys. Lett.*, **91**, 144105 (2007).
14. A.M. Schmidt, *Macromol. Rapid Commun*, **27**, 1168 (2006).
15. C. Velasco-Santos, A. Martinez-Hernandez, F.T. Fisher, R. Ruoff, and V.M. Castano, *Chem. Mater.*, **15**, 4470 (2003).
16. H.Z. Geng, R. Rosen, B. Zheng, H. Shimoda, L. Fleming, J. Liu, and O. Zhou, *Adv. Mater.*, **14**, 1387 (2002).
17. Y. Lin, B. Zhou, K.A.S. Fernando, P. Liu, L.F. Allard, and Y.P. Sun, *Macromolecules*, **36**, 7199 (2003).
18. M. Drubetski, A. Siegmann, and M. Narkis, *J. Mater. Sci.*, **42**, 1 (2007).
19. A. Dorigato, G. Giusti, F. Bondioli, and A. Pegoretti, *Expr. Pol. Lett.*, **7**, 673 (2013).
20. *J.C. Mol, J. Mol. Catal. A: Chem.*, **213**, 39 (2004).
21. C. Liu, S.B. Chun, P.T. Mather, L. Zheng, E.H. Haley, and E.B. Coughlin, *Macromolecules*, **35**, 9868 (2002).
22. M. Baba, J.L. Gardette, and J. Lacoste, *Polym. Degrad. Stab.*, **63**, 121 (1999).
23. M. Baba, S. George, J.L. Gardette, and J. Lacoste, *Polym. Int.*, **52**, 863 (2003).
24. T. Chung, A. Romo-Uribe, and P.T. Mather, *Macromolecules*, **41**, 184 (2008).
25. J. Leng, X. Lan, Y. Liu, and S. Du, *Prog. Mater. Sci.*, **56**, 1077 (2011).
26. M. Cuevas, J. Alonso, L. German, M. Iturrondobeitia, J.M. Laza, J.L. Vilas, and L.M. Leon, *Smart Mater. Struct.*, **18**, 1, (2009).
27. J. Kunzelman, T. Chung, P.T. Mather, and C. Weder, *J. Mater. Chem.*, **18**, 1082 (2008).
28. B. Likozar and M. Kranjinc, *Polym. Eng. Sci.*, **49**, 60 (2009).
29. J.E. Mark, *Physical Properties of Polymers Handbook*, Springer, New York (2007).
30. G. Rehage, *Pure Appl. Chem.*, **39**, 161 (1974).
31. D.I. Bower, *An Introduction to Polymer Physics*, Cambridge University Press, Cambridge (UK) (2002).
32. P.C. Painter and M.M. Coleman, *Essential of Polymer Science and Engineering*, DEStech Publications, Inc., Lancaster (USA) (2009).
33. A. Dorigato, M. D'Amato, and A. Pegoretti, *J. Polym. Res.*, **19**, 9889 (2012).
34. A. Dorigato, Y. Dzenis, and A. Pegoretti, *Mech. Mater.*, **61**, 79 (2013).
35. Q. Zhang, H. Liu, X. Wang, X. Shi, and X. Duan, *J. Wuhan Univ. Technol.*, **24**, 871 (2009).